

# Silk fibroin-sericin native blends as potential biomaterial templates

## Abstract

The silk produced by the domesticated silkworm (*Bombyx mori*) consists of two major polypeptidic components, fibroin and sericin. Both are used as biomaterial templates in tissue engineering applications, with variable success. While fibroin membranes are mechanically strong, they do not promote satisfactorily attachment and proliferation of cells. Sericin membranes display a precisely opposite behavior. In order to generate silk-based templates with optimal cell-adhesive properties and acceptable mechanical strength, we propose a method to manufacture fibroin-sericin blends in one single step, by processing the whole silk cocoons. The membranes prepared from these “native” blends were physically characterized in this study, and assessed as substrata for the growth of retinal photoreceptor cells. The antioxidant effect putatively inducible by sericin was also evaluated. The blend membranes were found to be mechanically stronger than the fibroin membranes and led to significant enhancement of cell proliferation. Our method also prevented the advanced hydrothermal degradation of fibroin and sericin during processing. The membranes displayed both excellent transparency and suitable water content. However, their permeability was low, and no antioxidative activity related to the presence of sericin was detected when oxidative stress was induced in the cell cultures. The method developed in this study provides silk-based membranes with improved characteristics for tissue engineering applications.

**Keywords:** *Bombyx mori* silk, fibroin, sericin, biomaterials, electrophoresis, FTIR analysis, cell proliferation, oxidative stress

Volume 5 Issue 1 - 2019

Shuko Suzuki,<sup>1</sup> Cassie L Rayner,<sup>1</sup> Traian V Chirila<sup>1-5</sup>

<sup>1</sup>Queensland Eye Institute, South Brisbane, Queensland, Australia

<sup>2</sup>Science & Engineering Faculty, Queensland University of Technology, Brisbane, Queensland, Australia

<sup>3</sup>Faculty of Medicine, University of Queensland, Herston, Queensland, Australia

<sup>4</sup>Australian Institute for Bioengineering and Nanotechnology, University of Queensland, Australia

<sup>5</sup>Faculty of Science, University of Western Australia, Crawley, Australia

**Correspondence:** Professor Traian V Chirila, Queensland Eye Institute, 140 Melbourne Street, South Brisbane, Queensland 4101, Australia, Tel 61-7-3239-5024, Email traian.chirila@qei.org.au

**Received:** February 05, 2019 | **Published:** February 12, 2019

## Introduction

Silks are natural proteinaceous materials, generally classified as fibrous proteins, which—in polymer terminology—shall be regarded as composites of assembled polypeptidic copolymer subunits. The silk produced by the larvae of the domesticated silk moth (*Bombyx mori*), the silkworm, has a long history of use by mankind, and is the most studied silk to date. *B. mori* silk consists of two major polypeptidic assemblies, known as fibroin (henceforth, BMSF) and sericin (BMSS), both isolable by physicochemical means. While BMSF has been extensively investigated as a biomaterial with applications in medicine,<sup>1-11</sup> BMSS has been reluctantly accepted as a biomaterial on account of a putative allergenic activity. We have analyzed exhaustively the existing publications on this topic, and have concluded that this opinion was rather speculative and based on either misinterpreted or misquoted previously reported results;<sup>12</sup> our conclusion has not only exonerated sericin from potential cytopathologic effects, but also substantiated similar findings reported either previously or subsequently.<sup>13-22</sup> Over the last decade, convincing evidence for sericin's biocompatibility has triggered wide interest in its potential applications as a biomaterial.<sup>23-27</sup>

Transition of silk from a textile commodity into a biomedical material is a development that has commenced less than three decades ago. Today the field of the biomedical applications of silk proteins is vast, although the number of regulatory-approved silk-based medical products for use in a clinical setting is still below the initial expectations. Both fibroin and sericin, predominantly those produced by *B. mori*, have been investigated and evaluated as templates (scaffolds, membranes, coatings) for tissue repair or replacement (e.g. bone and cartilage tissue engineering, bladder reconstruction, hepatic tissue engineering, vascular grafts, nerve repair), drug or gene

delivery, cell encapsulation and delivery, tissue adhesives, and wound dressing. The review articles cited above offer detailed accounts of the biomedical applications involving BMSF or BMSS.

Our research group was the first to assess the response to silk proteins of different cells and tissues of the eye.<sup>4,12,28-31</sup> We have shown that the attachment of human corneal limbal epithelial cells to BMSS membranous templates was superior to the attachment to identical BMSF substrata.<sup>12</sup> Mixing sericin with fibroin, each isolated as individual materials, was detrimental to the attachment of cells. However, while the membranes made of pure BMSS, or of BMSS blended with less than 10% BMSF, displayed enhanced cell-adhesive characteristics, their mechanical properties were inferior to BMSF, such precluding an optimal surgical handling of the cell–substratum constructs in tissue engineering applications.

A limitation to the use of silk proteins is related to their isolation from silk cocoons. The methods to isolate fibroin and sericin from silk cocoons are generally based on differential solubility. Methods that do not require elevated temperatures include the dissolution of these proteins in organic solvents, or their salt-mediated solubilization. There are only a few organic solvents able to dissolve silk proteins; all being toxic or very toxic, they are seldom used. Concentrated aqueous solutions of lithium halides and a few other salts of alkaline and alkaline earth metals proved to be powerful solubilizing agents for both fibroin and sericin at ambient temperature. However, most of the current procedures, especially those aiming at separating BMSF from BMSS, involve temperatures in the vicinity of the boiling temperature of water. In these conditions, both proteins undergo significant hydrothermal degradation resulting in non-uniform mixtures of undefined polypeptides with molecular masses lower, or much lower, than the components of silk in their native state. We have shown<sup>32</sup>

that the hydrothermally induced fragmentation of BMSS during the isolation procedure can be significantly reduced through the use of long-duration aqueous extraction at temperatures not surpassing 50°C.

The aim of the study was to develop a method to create silk-based templates that combine the good cell-adhesive properties of sericin with the mechanical strength of fibroin, while also displaying minor alteration of the molecular mass size and distribution. For this purpose, we investigated the process of dissolving the whole silk cocoons in mild conditions in order to preserve the native quantitative ratio between BMSF and BMSS. Such compositions, which henceforth will be called “native blends”, were fashioned into membranes that were then characterized as potential biomaterial templates for tissue engineering applications.

## Materials and methods

### Materials

*B. mori* cocoons, with the pupae removed, were supplied by Tajima Shoji Co. Ltd. (Yokohama, Japan). All chemical reagents were supplied by Sigma-Aldrich (St Louis, MO, USA). In all experiments, high-purity water (Milli-Q or equivalent) was used. Minisart®-GF pre-filters (0.7 µm) and Minisart® High-Flow filters (0.2 µm) were purchased from Sartorius Stedim Biotech (Göttingen, Germany). The dialysis tubes with a molecular-mass cut-off (MMCO) of 12.4 kDa were supplied by Sigma-Aldrich. The olefin copolymer Topas® 8007S-04 was supplied by Advanced Polymers (Frankfurt, Germany). All cell culture reagents and supplements were purchased from Life Technologies (Mulgrave, Victoria, Australia), except for the foetal bovine serum (FBS), which was supplied by Thermo Scientific (Rockford, IL, USA). Ethanol 70% v/v for sterilization was prepared from absolute ethanol purchased from Chem-Supply (Port Adelaide, South Australia, Australia). The 661W murine retinal photoreceptor line has originated in Professor Muayyad Al-Ubaidi's laboratories (University of Oklahoma), and was kindly provided to us by Dr. Krisztina Valter-Kocs (Australian National University, Canberra).

### Isolation of BMSF and preparation of BMSF membranes

Solutions of BMSF were prepared according to a slightly modified protocol previously reported.<sup>28</sup> Briefly, the sericin component was removed by boiling the cocoons in an aqueous solution of sodium carbonate (the “degumming” stage), followed by washings, drying, dissolution in concentrated lithium bromide, filtering, and dialysis. The concentration of solutions was adjusted to approximately 1.8% w/w (checked gravimetrically), and membranes were cast from these solutions. In order to water-anneal the membranes, the dishes containing dried membranes were then placed in a vacuum enclosure together with a container filled with water. A vacuum of -80 kPa was applied and the materials were maintained under vacuum, at room temperature, for 24 h. After the treatment, the thickness of the membranes was around 10 µm.

### Preparation of the native blend BMSF/BMSS solutions and membranes

The silk cocoons were dissolved in a concentrated buffered lithium bromide (LiBr) solution (pH 9). Published protocols,<sup>33,34</sup> have been followed with some modifications. Cut cocoons (1.5 g) were soaked in 70% ethanol (3.75 mL, or 1/20 of the final volume designated to be 75 mL) for 5 min. It was asserted<sup>34</sup> that this operation enhanced the

permeation of LiBr solution into the cocoon layers by reducing surface tension. Then, 71.25 mL of a solution of 9.5 M LiBr in 0.1 M Tris-HCl buffer (pH 9) was added to bring up the final concentration of the cocoon material to 20 mg/mL, while also assuring a concentration of no less than 9 M LiBr in the final solution. The mixture was stirred either at room temperature, or at 50°C for 24 h, in order to obtain two different blends. The solutions were then centrifuged at 14,500 rpm for 10 min to remove the insoluble matter. Each resulting solution was placed in dialysis tubing with MMCO 12.4 kDa, and dialyzed against 5 L of water for 3 days with 2 water exchanges/day. The solution was removed from the tube, centrifuged and collected in a container that was stored at 4°C until further use. Henceforward, the native blend processed at room temperature is codenamed as F/S#1, while that processed at 50°C is codenamed as F/S#2. The concentration of silk proteins in the two final solutions, after dialysis, was in the range of 0.8 to 0.9% w/w, as determined by gravimetric analysis. Free-standing membranes for further evaluation were cast in 5-cm diameter polymer (Topas®)-coated Petri dishes from a solution with a residual content of dry protein of 1.8 mg/cm<sup>2</sup>, while the wells of a 24-well plate were coated with films resulting from a solution containing 1.4 mg/cm<sup>2</sup> dry protein content. After being subjected to water-annealing, as described in the previous section, the membranes were peeled from the supporting surfaces and used in further experiments. Their thickness was approximately 10 µm. The amounts of dissolved silk proteins in LiBr solutions were quantified using the bicinchoninic acid (BCA) assay. A Micro BCA protein assay kit supplied by Thermo Scientific (Rockford, IL, USA) was employed and the manufacturer's protocol was followed strictly. After centrifugation, the solutions were diluted 1000 times with water. As standard samples for the calibration curve, BMSF solution (3%), diluted with 9.5 mM LiBr, was employed after adjusting the concentration to various values within the range 0.5 to 200 µg/mL.

### Gel-electrophoretic analysis of BMSF/BMSS native blends

The distribution and size of the molecular mass in the native blends F/S#1 and F/S#2, and in BMSF (for a comparison), were investigated by sodium dodecyl sulfate-polyacrylamide gel electrophoresis (SDS-PAGE), using a Novex® XCell Sure Lock™ Mini-Cell system (Life Technologies Inc., Carlsbad CA, USA), with an EPS-250 Series II Power Supply unit (CBS Scientific Co. Inc., San Diego, CA, USA). The protocol detailed in a previous report<sup>32</sup> was followed in all aspects.

### Analysis by FTIR-ATR spectrometry

The Fourier-transform infrared spectra of the F/S#1 and F/S#2 blends and of BMSF were collected and recorded in a Nicolet Nexus 5700 FTIR spectrometer (Thermo Electron Corp., Marietta, OH, USA), equipped with the Nicolet Smart Endurance diamond attenuated total reflectance accessory (ATR). The spectra were processed by the co-addition of 64 scans in the range 4000 to 525 cm<sup>-1</sup>, at a resolution of 8 cm<sup>-1</sup>. The OMNIC 7 (Thermo Electron Corp.) software package was employed for recording and analyzing the spectra.

### Physical characterization of BMSF/BMSS native blends as biomaterials

**Transparency:** As the transparency of cell-biomaterial constructs is generally relevant to clinical applications in ophthalmology, the light transmission of the membranes (F/S#1, F/S#2 and BMSF) was measured at a wavelength of 550 nm using the microplate spectrometer AC200D (Paradigm Absorbance Detection, Beckman

Coulter, Brea, CA, USA). The membranes were cut into 6-mm diameter discs and placed in the wells of a 96-well plate; 200 µL of phosphate buffered saline (PBS) was added to each well, and the plate was kept at room temperature for 1 h. The transmission of 550-nm visible radiation through the membranes was measured at room temperature, on triplicate samples, and the control background was defined by PBS alone.

**Microscopic morphology:** Microstructural features seen through the bulk of the F/S#1, F/S#2 and BMSF, as dried membranes, were examined on a bright-field Nikon Eclipse® TS100 microscope (Nikon Corp., Tokyo, Japan), equipped with a Nikon Digital Sight camera, and using the NIS Elements® F4.00.00 software.

**Permeability:** The permeability of all membranes was examined in a horizontal diffusion cell, consisting of 2 stirred reservoirs linked through a 19-mm diameter tube, and employing a red azo dye, disodium 6-hydroxy-5-[(2-methoxy-5-methyl-4-sulfonatophenyl)diazaryl]naphthalene-2-sulfonate, known as Allura Red AC, as a test molecule (molar mass 496.42 g/mol), according to a previously established protocol.<sup>35</sup> Briefly, the membrane was clamped watertight across the cross-section of the tube, and one chamber was filled with a PBS-buffered solution of Allura Red AC, and the other with PBS only. Samples (100µL) were periodically withdrawn from the chamber filled with PBS only, and the absorbance at 504nm was measured using the microplate spectrophotometer Beckman Coulter AC200D to determine the concentration of Allura Red AC and then to calculate its permeability coefficients. The coefficients are reported as results of triplicate measurements.

**Equilibrium water content:** Membrane samples (about 1 cm<sup>2</sup> in area) were soaked in water at 37°C for 1 h and weighed following removal of excess surface water by blotting with tissue paper. The samples were dried in an oven at 90 °C overnight, and weighed again to record their dry weights. The equilibrium water content (EWC), as weight percentage, was calculated using Equation (1), where  $W_{\text{wet}}$  and  $W_{\text{dry}}$  are the weights of hydrated and dried same sample, respectively.

$$\text{EWC}(\%) = \frac{(W_{\text{wet}} - W_{\text{dry}})}{W_{\text{wet}}} \times 100 \quad (1)$$

The values are reported as results of 6 measurements for each sample.

**Mechanical testing:** Strips (1 x 3 cm) cut out from each of the membranes were subjected to tensile measurements using an Instron Materials Testing System, Model 5943 (Instron, Norwood, MA), equipped with a 50-N load cell, at a crosshead speed of 14 mm/min. The strips were loaded by pneumatic grips, which were set to a gauge distance of 14 mm, and soaked in PBS buffer (pre-heated to 37 ± 3°C) in a BioPuls™ unit for 5 min prior to stretching. Stress-strain plots were recorded and Young's modulus was determined from the slope of the linear region of the curve. The mean values were calculated from six measurements for each membrane.

### Cell proliferation and oxidative stress assays

The 661W retinal photoreceptor cells were initially established in T75 tissue culture flasks in Dulbecco modified Eagle's medium (DMEM) supplemented with 10% FBS, 2 mM L-glutamine and 50 U/ml penicillin/50 mg/ml streptomycin [36]. After harvesting, cells were seeded into 24-well plates pre-coated with silk protein membranes (6 specimens for each membrane), at a density of 5,000 cells per well. Uncoated wells (tissue culture plastic, TCP) served as controls. Cells

were allowed to adhere and proliferate for 24 h before reducing the serum concentration to 5% FBS and culturing for a further 5 days. The reduction of the blue dye resazurin assay was then applied to quantify cell viability. Briefly, 70 mM resazurin (7-hydroxy-10-oxido phenoxazin-10-iun-3-one, known also as Alamar Blue) stock solutions were prepared in Hank's balanced salt solution (HBSS), filter-sterilized (0.2-µm filter), and stored at -40°C until required. Prior to running the assay, the stock solution was diluted 1:100 in culture medium supplemented with 1% FBS, to achieve a 700 µM working solution. Exhausted media were aspirated, 1 mL of resazurin dye solution added to each well, and the cells incubated for 3 h at 37°C. After that, the absorbance of each sample was measured at 570 nm (for the reduced form) and 600 nm (for the oxidized form) in the Beckman Coulter AC200D microplate spectrophotometer. Equation (2) was used to convert absorbance readings to the percentage of the reduction of resazurin to resofurin.<sup>37</sup>

$$\% \text{ Reduction} = \frac{(117,216 \times A_{570}) - (80,586 \times A_{600})}{(155,677 \times A'_{600}) - (14,652 \times A'_{570})} \times 100 \quad (2)$$

In this equation, 117,216 is the molar extinction coefficient of resazurin (oxidized form) at 600 nm; 80,586 is the molar extinction coefficient of resazurin at 570 nm; 14,652 is the molar extinction coefficient of resofurin (reduced form) at 600 nm; 155,677 is the molar extinction coefficient of resofurin at 570 nm;  $A_{600}$  is the absorbance of test wells at 600 nm;  $A_{570}$  is the absorbance of test wells at 570 nm;  $A'_{600}$  is the absorbance of negative control wells at 600 nm; and  $A'_{570}$  is the absorbance of negative control wells at 570 nm.

Oxidative stress assays were conducted after 5 days of culture on each silk membrane (6 specimens for each membrane). Within each treatment group, 3 wells served as controls and 3 were treated with the pro-oxidant, *tert*-butyl hydroperoxide (*t*BuOOH). The cells were treated with either 300 µM of *t*BuOOH solution or 1% FBS vehicle control for 3 h. Following the stress-inducing treatment, the medium was removed and the cells washed briefly with Dulbecco's phosphate buffered saline (DPBS) to remove all traces of oxidant. Resazurin assays were performed as described previously and the percent reduction calculated. The degree of oxidative induced stress/damage was determined by comparing stressed with non-stressed wells

The proliferation and oxidative stress assays were conducted in sextuplet or triplicate, respectively, for two series of experiments. Bright-field microscopy was used to visualize and photograph 5-day cell cultures on a Nikon Eclipse® TS100 microscope, equipped with a Nikon Digital Sight camera, and using the NIS Elements® F4.00.00 software.

### Statistic analysis

The results in this study were processed statistically using Version 6.0 of the GraphPad Prism® software. For parametric tests (EWC, tensile testing and cell proliferation experiments), the one-way analysis of variance (ANOVA) in conjunction with Tukey-Kramer multiple comparisons was employed. Kruskal-Wallis test was used for nonparametric tests (transmittance and permeability).

## Results and discussion

### Molecular mass distribution

The BCA assay showed that the maximum solubility of total polypeptidic components in the LiBr solution, before dialysis, was 87% when dissolution was carried out at room temperature, and 92%

when the cocoon material was dissolved at 50°C. The electrophoretic mobility of the polypeptidic components in the dialyzed solutions (BMSF, F/S#1, and F/S#2) was investigated by SDS-PAGE.

Figure 1 shows the distribution patterns presented by the three solutions. While BMSF, isolated in a process involving a higher temperature, revealed a smear pattern indicative of advanced hydrothermal degradation, the two native blend solutions showed considerably less degradation. Based on previously reported analyses,<sup>33,38,39</sup> we identified two (or more) high molecular mass (over 400 kDa) components belonging to sericin and fibroin (Figure 1). However, the sericin band in F/S#2 appears depleted, likely due to a higher processing temperature; indeed, we have shown previously<sup>32</sup> that even a temperature of 50°C can induce the hydrothermal degradation of sericin (Figure 2).

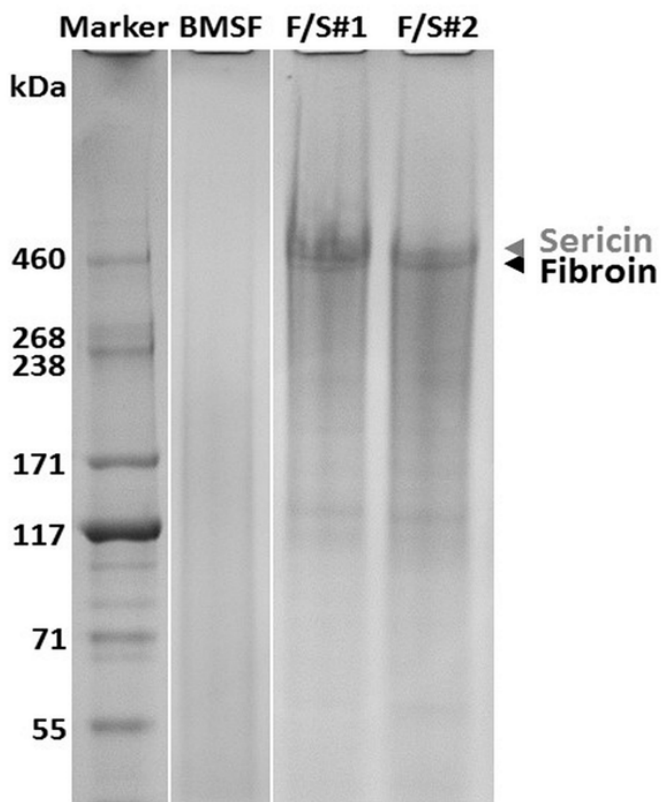


**Figure 1** Electrophoretic patterns of BMSF, F/S#1 and F/S#2 solutions.

#### Effect of water annealing on the secondary structure of silk

In order to render the membranes insoluble, they were subjected to water annealing. The ‘Amide I’ region in the infrared spectra (approximately from 1590 to 1720 cm<sup>-1</sup>) was selected to monitor the formation of the insoluble antiparallel β-sheet crystalline conformation and the simultaneous reduction of the silk’s soluble regions consisting of random coil and α-helix conformations, both induced by the water-annealing process. In Figure 2, it can be seen that following water annealing, new absorption peaks characteristic to the β-sheet conformations were generated at the wavenumbers 1622 and 1700 cm<sup>-1</sup>, while the absorption due to non-crystalline α-helix (at 1645 cm<sup>-1</sup>) and, in particular, random coil conformations (centered at 1636 cm<sup>-1</sup>) were dramatically reduced. Our findings confirm other previous results on the effect of water annealing on silk structure.<sup>40</sup> In

the F/S#1 and F/S#2 blends, a more emphatic predominance of the β-sheet crystalline region was observed as compared to BMSF, which has been reported<sup>41</sup> for blends with high sericin contents.

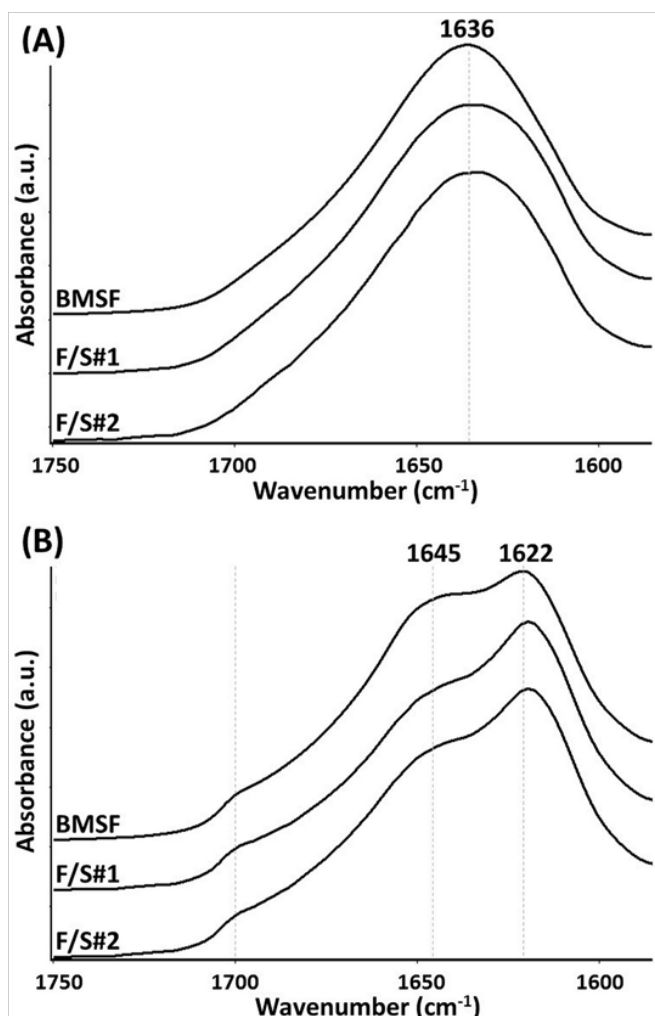


**Figure 2** The Amide I region in the FTIR spectra of fibroin and native blend membranes before water annealing (A) and after water annealing (B).

#### Physical properties of the membranes

Transparency of membranes was evaluated by measuring the transmission of 550-nm-wavelength visible light.

As seen in Figure 3, all membranes displayed superior transparency, significantly higher than that of the natural human cornea<sup>42,43</sup> or of the amniotic membrane,<sup>44</sup> currently the substratum most frequently used for the tissue-engineered repair of the ocular surface. Between them, BMSF showed higher transparency than F/S#1 or F/S#2. A reason for a decreased transparency of the blend membranes could be the presence of microscopic irregularities able to cause diffuse reflectance of the incident light, which would strongly suggest phase separation. Indeed, the microscopic examination of the bulk material in BMSF, F/S#1 and F/S#2 clearly indicated phase separation in the blends, while pure fibroin was relatively homogeneous (Figure 4).

The phase separation in the blends can be explained by the poor physical compatibility between fibroin and sericin, which has been first evidenced through differential scanning calorimetry and transmission electron microscopy,<sup>13</sup> and it is likely one of the consequences of the

significant difference between the amino acid compositions of the two proteins. For instance, the contents of amino acids with polar side chains and of acidic amino acids in sericin are about three times, and respectively five times, higher than in fibroin.<sup>13</sup> We shall recall that the blends of this study are “native” only in that they preserve the global quantitative ratio between fibroin and sericin, while—in reality—fibroin and sericin never mix intimately in the natural *B. mori* cocoons, where the fibroin filaments (the so-called “brins”) in each thread are coated and glued in pairs by sericin. Fibroin is produced in the posterior gland of the silkworm, but sericin is produced in the middle silk gland and builds up in three successive layers that envelop the fibroin filaments.<sup>45–47</sup> It was suggested<sup>41</sup> that the physical incompatibility between fibroin and sericin may be in fact the result of a natural evolutionary process where the ensuing phase separation prevents the solidification of fibroin prior to the spinning of silk thread from the silkworm’s middle silk gland. The level of phase separation in F/S#2 appear to be higher than in F/S#1 (Figure 4), probably due to a higher level of degradative fragmentation during the processing of F/S#2, as suggested in Figure 1. In this study, other characteristics important for a biomaterial, such as the permeability and water content of the

membranes, were also estimated. Permeability to an organic molecule with a molecular mass of about 0.5 kDa is shown in Figure 5.

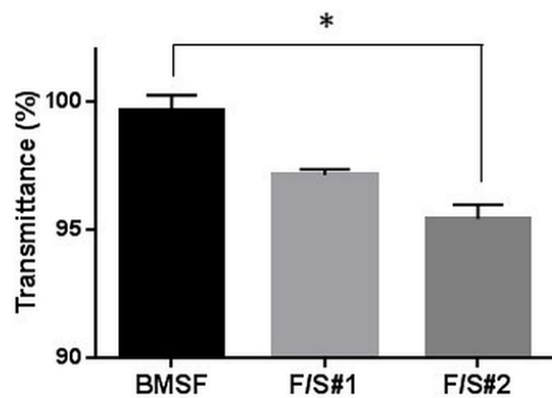


**Figure 3** Light transmittance of hydrated membranes at the wavelength of 550 nm. The bars represent mean values  $\pm$  s.d. resulting from three different measurements. \*  $p < 0.05$ .

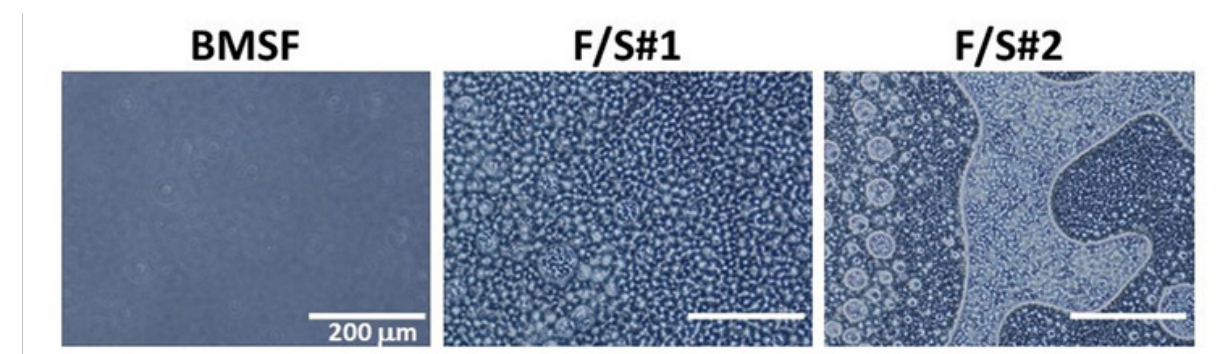


**Figure 4** Light micrographs of the dried membranes.

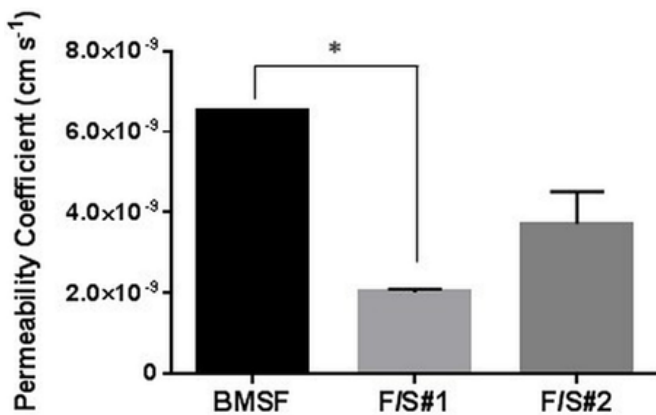


**Figure 5** Permeability of membranes to Allura Red AC. The bars represent mean values  $\pm$  s.d. resulting from three separate measurements. \*  $p < 0.05$ .

Both native blend membranes showed markedly less permeability than the fibroin membranes (Figure 5). The value for BMSF is similar to that reported by us elsewhere<sup>48</sup> for a sample processed in slightly different conditions. It is difficult to explain why the permeability of F/S#2 is higher than that of F/S#1, unless it may be related to the phase separation. Suitable permeability of biomaterial templates has physiological significance both in the form of substrata for cell growth and as implants, allowing transport of nutrients, oxygen, waste products and cell-signalling molecules. The permeability of silk-

based membranes, as estimated in this study and as reported by others, is inferior to the natural cornea, sclera or conjunctiva.<sup>49</sup>

The equilibrium water content (EWC) of BMSF and of native blend membrane materials is shown in Figure 6, and the values are typical of the hydrogels used in biomedical applications. The trend of EWC increasing from fibroin towards the F/S blends is explained by a higher inherent hydrophilicity of sericin as compared to fibroin. The highest EWC as determined for F/S#2 may be related to the phase separation that can induce within the internal architecture of the gel pore-like pathways and local reservoirs for the penetration and storage of water. Evaluation of the tensile properties of membranes were made after the samples, as solid films, were stored in PBS for 5 min in the BioPuls™ unit attached to the mechanical tester. The samples were only partially hydrated, but a compromise was necessary as we found that the fully hydrated membrane were too weak to enable proper fixation within the pneumatic grips of the tester. The investigation of mechanical properties revealed unexpected results. In a previous report,<sup>12</sup> we have shown that the mechanical characteristics (strength, stiffness, and elasticity) were very poor in membranes made from sericin, or from blends of sericin with fibroin, with the experimentally measured values being much lower than those for BMSF. Importantly, those particular blends were made by mixing variable proportions of solutions of BMSF and BMSS, each of them having been isolated independently by specific methods that involved processing at higher temperatures. The present study followed a different scenario. By processing the whole cocoons in mild conditions and without prior

individual isolation of BMSF or BMSS, the resulting “native” blends generated membranes with mechanical properties superior to those of BMSF, as shown in Figure 7. An explanation may tentatively be based on the more advanced hydrothermal degradation of BMSF when conventional procedures were employed for its isolation. When compared between them, the mechanical properties of F/S#2 membranes are inferior to those of F/S#1 membranes, albeit they are still stronger than the BMSF membranes. We tentatively explain this by the higher water content and enhanced phase separation in F/S#2. To our knowledge, this finding is the first observation related to the advantage of obtaining stronger fibroin-sericin membranes by processing whole silk cocoons, rather than isolating in advance each protein component and subsequently mixing them.

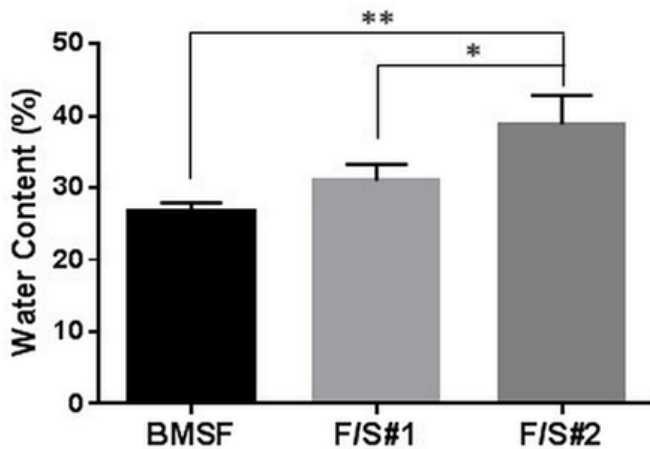


**Figure 6** The equilibrium water content of fully hydrated membranes. The bars represent mean values  $\pm$  s.d. resulting from six separate measurements. \*  $p < 0.001$  and \*\*  $p < 0.0001$ .

### Cell proliferation and oxidative stress assays

The cells from a murine line (661W) of retinal photoreceptor cells were selected for assessing cell proliferation on the membranes produced in this study. The photoreceptor cells of the retina are of crucial importance for the visual processes in the eye, and they are particularly sensitive to damage from oxidative stress. As expected, the sericin's presence in the F/S#1 and F/S#2 membranes induced a statistically significant enhancement of cell proliferation relative to the BMSF membrane (Figure 8), confirming our previous findings.<sup>12</sup> Here, the number of viable cells after 5 days in culture was expressed indirectly by the percentage reduction of resazurin to resorufin according to the Alamar Blue cell viability assay. The viable cells convert continuously resazurin to resorufin, therefore less percentage of reduction represents less viable cells. The advantage of the method is that the cells remain viable after the assay and can be subjected to further analysis.

The microscopic examination of the proliferating cells (Figure 9) confirms a satisfactory performance of the F/S#1 membrane as a substratum for growing cells, and also suggests phase separation as a possible reason for the poorer performance of the F/S#2 membrane. However, it is not known whether the fibroin-sericin ratio plays a role, if any, in the enhancement of cell attachment. Neither we know whether this ratio is close to the natural ratio in *B. mori* silk thread (approximately 70–75% fibroin to 25–30% sericin), as to determine this ratio was beyond the purpose of our study. Since some sericinoid peptides with low molecular mass can dissolve in water and be washed away during processing, we may expect that the ratio in the “native” blends may shift in favour of fibroin.

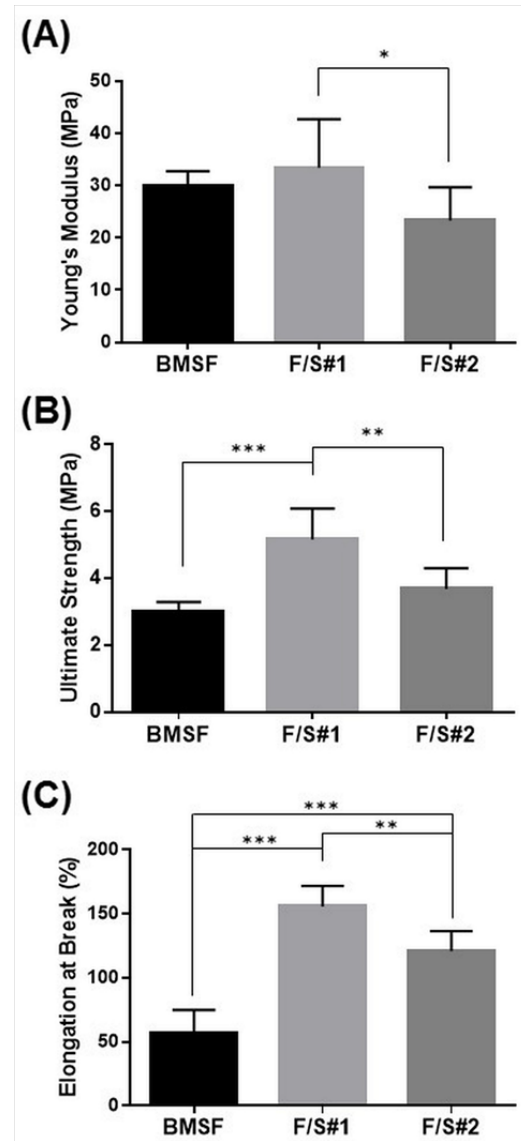


**Figure 7** Tensile characteristics of membranes: (A) Young's modulus; (B) Ultimate tensile strength; (C) Elongation at break. The bars represent mean values  $\pm$  s.d. resulting from six separate measurements. \*  $p < 0.05$ , \*\*  $p < 0.01$  and \*\*\*  $p < 0.0001$ .

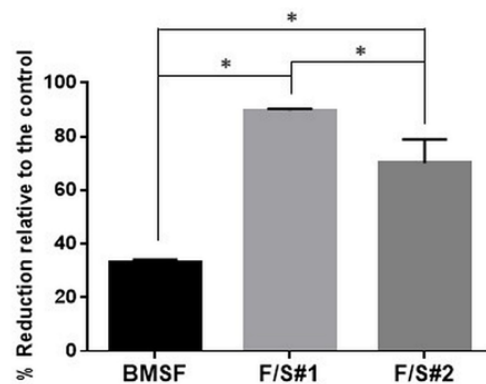


**Figure 8** Metabolic activity of murine photoreceptor cells (661W) on membranes after 5 days of culture. The bars represent percentages of resazurin reduced to resorufin as compared with the TCP control (assumed to correspond to 100% completion of the reduction process) as mean values  $\pm$  s.d. resulting from two assays with six separate measurements per assay. \*  $p < 0.0001$ .

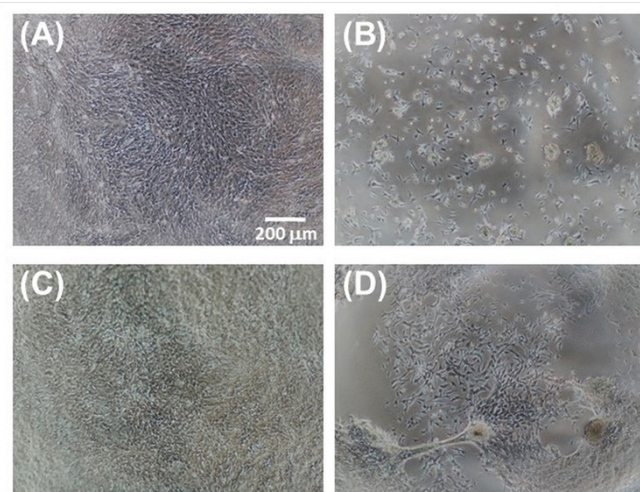


**Figure 9** Microscopic images of 661W cells grown on various membranes after 5 days of culture: (A) TCP control; (B) BMSF; (C) F/S#1; and (D) F/S#2.

Since we have previously demonstrated<sup>12</sup> that the blend membranes made by mixing individually isolated BMSF and BMSS displayed poor cell attachment when BMSF was quantitatively predominant, the finding in our current study is rather intriguing. Improved cell adhesion may be, simply, a consequence of less degradation of the two polypeptidic assemblies, fibroin and sericin.

Our investigation of a potential antioxidant effect of the sericin, was prompted by a growing literature, albeit not always relevant, on the antioxidative, enzyme-inhibiting, or cytoprotective effects of sericin produced by various silkworm species. Sericin as such was reported as an antioxidant either in the form of a solid powder or in aqueous solutions.<sup>50–58</sup> However, some investigators noticed such effects only in the extracts likely containing mainly non-sericinoid substances,<sup>59,60</sup> while others reported them both in sericin and in its extracts.<sup>61,62</sup> As shown in Figure 10, the presence of sericin in the composition of the substrata does not have any effect upon the number of cells remaining viable after oxidative stress was applied to the cultures.

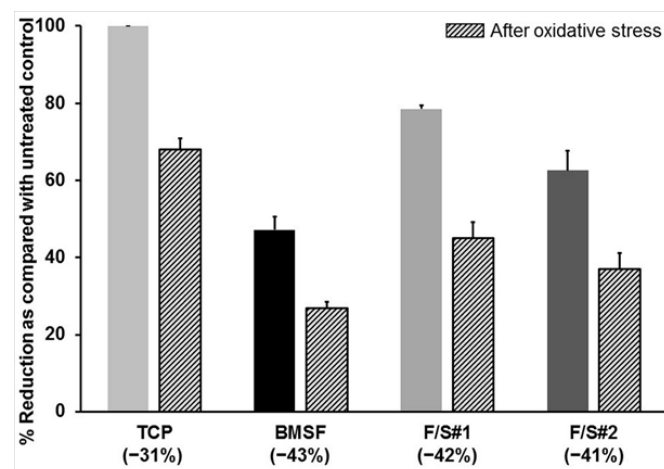


**Figure 10** Viability of cells prior to and after the application of oxidative stress. Cells grown on membranes for 5 days were treated with a pro-oxidant (tert-butyl hydroperoxide), and the resazurin assay was performed before and after this treatment. Percent of resazurin that was reduced to resorufin, shown on y-axis, is directly related to the numbers of viable cells. The bars represent mean values  $\pm$  s.d. resulting from two assays with three separate measurements in each. Percentage values in brackets along the x-axis indicate the drop in cells numbers as a consequence of oxidative stress induced by pro-oxidant.

The number of viable cells decreased by approximately the same amount in cultures grown on the BMSF, F/S#1 or F/S#2 membranes. The least depletion in cell numbers was actually on the TCP substrata (controls), where no external antioxidative protection was available beside the well-known cells' own defense mechanisms, including damage removal and repair system, transient growth-arrest, transient adaptive responses, modulation of gene expression, and utilization of natural antioxidants (e.g. vitamins E and C, uric acid, glutathione, etc.).<sup>63</sup> Although the same defense mechanisms would have been available to the cells growing on the sericin-containing membranes, our results show a decline in the prevention of cell death due to oxidative stress, and therefore cannot confirm an effective antioxidant activity attributable to sericin.

## Conclusions

The processing in mild conditions of whole silk cocoons affords fibroin-sericin blends from which membranes can be produced that display high transparency, improved mechanical properties, and enhanced cell proliferation. Compared to membranes made of fibroin alone, or resulting from blends of fibroin and sericin isolated individually prior to mixing, the membranes reported in this study suggest superior performance as biomaterial templates for tissue engineering applications. However, no antioxidant activity can be attributed to the presence of sericin.

## Acknowledgments

The authors thank Dr. Katsura Kojima (National Agriculture and Food Research Organization, Tsukuba, Japan) for constructive discussions and advice. This research was funded by an unrestricted grant provided by the Queensland Eye Institute Foundation, Australia, through Viertel's Vision Program.

## Conflicts of interest

The authors declare no conflicts of interest.

## References

- Vepari C, Kaplan DL. Silk as a biomaterial. *Prog Polym Sci.* 2007;32(8):991–1007.
- Hakimi O, Knight DP, Vollrath F, et al. Spider and mulberry silkworm silks as compatible biomaterials. *Composites B.* 2007;38(3):324–337.
- Murphy AR, Kaplan DL. Biomedical applications of chemically-modified silk fibroin. *J Mater Chem.* 2009;19:6443–6450.
- Harkin DG, George KA, Madden PW, et al. Silk fibroin in ocular tissue reconstruction. *Biomaterials.* 2011;32:2445–2458.
- Wenk E, Merkle HP, Meinel L. Silk fibroin as a vehicle for drug delivery applications. *J Control Rel.* 2011;150:128–141.
- Kundu B, Rajkhowa R, Kundu SC, et al. Silk fibroin biomaterials for tissue regenerations. *Adv Drug Deliv Rev.* 2013;65(4):457–470.
- Kundu B, Kurland NE, Bano S, et al. Silk proteins for biomedical applications: bioengineering perspectives. *Prog Polym Sci.* 2014;39(2):251–267.
- Patra C, Engel FB. Silk for cardiac tissue engineering. In Kundu SC, editor. *Silk Biomaterials for Tissue Engineering and Regenerative Medicine.* Amsterdam: Elsevier; 2014. p. 429–455.
- Hodgkinson AT, Bayat A. Silk for dermal tissue engineering. In Kundu SC, editor. *Silk Biomaterials for Tissue Engineering and Regenerative Medicine.* Amsterdam: Elsevier; 2014. p. 456–471.
- Yucel T, Lovett ML, Kaplan DL. Silk-based biomaterials for sustained drug delivery. *J. Control Rel.* 2014;190:381–397.

11. Kapoor S, Kundu SC. Silk protein-based hydrogels: Promising advanced materials for biomedical applications. *Acta Biomater.* 2016;31:17–32.
12. Chirila TV, Suzuki S, Bray LJ, et al. Evaluation of silk sericin as a biomaterial: in vitro growth of human corneal limbal epithelial cells on *Bombyx mori* sericin membranes. *Prog Biomater.* 2013;2(1):14.
13. Minoura N, Aiba S, Gotoh Y, et al. Attachment and growth of cultured fibroblast cells on silk protein matrices. *J Biomed Mater Res.* 1995;29(10):1215–1221.
14. Panilaitis B, Altman GH, Chen J. Macrophage responses to silk. *Biomaterials.* 2003;24(18):3079–3085.
15. Terada S, Sasaki M, Yanagihara K, Yamada H. Preparation of silk protein sericin as mitogenic factor for better mammalian cell culture. *J Biosci Bioeng.* 2005;100(6):667–671.
16. Tsubouchi K, Igarashi Y, Takasu Y, et al. Sericin enhances attachment of cultured human skin fibroblasts. *Biosci Biotechnol Biochem.* 2005;69(2):403–405.
17. Teramoto H, Kameda T, Tamada Y. Preparation of gel film from *Bombyx mori* silk sericin and its characterization as a wound dressing. *Biosci Biotechnol Biochem.* 2008;72(12):3189–3196.
18. Aramwit P, Kanokpanont S, De-Eknamkul W, et al. The effect of sericin with variable amino-acid content from different silk strains on the production of collagen and nitric oxide. *J Biomater Sci Polym Ed.* 2009;20(9):1295–1306.
19. Aramwit P, Kanokpanont S, De-Eknamkul W, Srichana T. Monitoring of inflammatory mediators induced by silk sericin. *J Biosci Bioeng.* 2009;107(5):556–561.
20. Hakimi O, Gheysens T, Vollrath F, et al. Modulation of cell growth on exposure to silkworm and spider silk fibers. *J Biomed Mater Res.* 2010;92(4):1366–1372.
21. Aramwit P. Bio-response to silk sericin. In Kundu SC, editor. *Silk Biomaterials for Tissue Engineering and Regenerative Medicine.* Amsterdam: Elsevier; 2014. p. 299–329.
22. Rocha LKH, Favaro LIL, Rios AC, et al. Sericin from *Bombyx mori* cocoons. Part I: Extraction and physicochemical–biological characterization for biopharmaceutical applications. *Process Biochem.* 2017;61:163–177.
23. Kundu SC, Dash BC, Dash R, et al. Natural protective glue protein, sericin bioengineered by silkworms: potential for biomedical and biotechnological applications. *Prog Polym Sci.* 2008;33:998–1012.
24. Khan MMR, Tsukada M. Electrospun silk sericin nanofibers for biomedical applications. In Kundu SC, editor. *Silk Biomaterials for Tissue Engineering and Regenerative Medicine.* Amsterdam: Elsevier; 2014. p. 125–156.
25. Wang Z, Zhang Y, Zhang J, et al. Exploring natural silk protein sericin for regenerative medicine: an injectable, photoluminescent, cell-adhesive 3D hydrogel. *Sci Rep.* 2014;4:7064.
26. Lamboni L, Gauthier M, Yang G, et al. Silk sericin: A versatile material for tissue engineering and drug delivery. *Biotechnol Adv.* 2015;33(8):1855–1867.
27. Cao TT, Zhang YQ. Processing and characterization of silk sericin from *Bombyx mori* and its application in biomaterials and biomedicines. *Mater Sci Eng C.* 2016;61:940–952.
28. Chirila TV, Barnard Z, Zainuddin, et al. *Bombyx mori* silk fibroin membranes as potential substrata for epithelial constructs used in the management of ocular surface disorders. *Tissue Eng A.* 2008;14(7):1203–1211.
29. Madden PW, Lai JNX, George KA, et al. Human corneal endothelial cell growth on a silk fibroin membrane. *Biomaterials.* 2011;32(17):4076–4084.
30. Chirila TV, Suzuki S, Hirst LW, et al. Reconstruction of the ocular surface using biomaterial templates. In Chirila TV, Harkin DG, editors. *Biomaterials and Regenerative Medicine in Ophthalmology*, 2<sup>nd</sup> edn. Amsterdam: Elsevier; 2016. p. 179–218.
31. Shadforth AMA, Chirila TV, Harkin DG, et al. Biomaterial templates for the culture and transplantation of retinal pigment epithelial cells: A critical review. In Chirila TV, Harkin DG, editors. *Biomaterials and Regenerative Medicine in Ophthalmology*, 2<sup>nd</sup> edn. Amsterdam: Elsevier; 2016. p. 263–289.
32. Chirila TV, Suzuki S, McKirdy NC. Further development of silk sericin as a biomaterial: comparative investigation of the procedures for its isolation from *Bombyx mori* silk cocoons. *Prog Biomater.* 2016;5:135–145.
33. Murakami M, Tamada Y, Kojima K. Dissolving whole cocoon silk proteins by using a pH-adjusted buffered LiBr solution [in Japanese]. *Nippon Silk Gakkaishi.* 2012;20:89–94.
34. Kojima K, Murakami M, Tamada Y. Optimization of pretreatment and LiBr concentration for dissolving whole cocoon silk proteins [in Japanese]. *Nippon Silk Gakkaishi.* 2013;21:45–47.
35. Bray LJ, George KA, Ainscough SL, et al. Human corneal epithelial equivalents constructed on *Bombyx mori* silk fibroin membranes. *Biomaterials.* 2011;32(22):5086–5091.
36. Rayner CL, Bottle SE, Gole GA, et al. Real-time quantification of oxidative stress and the protective effect of nitroxide antioxidants. *Neurochem Int.* 2016;92:1–12.
37. Larson EM, Doughman DJ, Gregerson DS, et al. A new, simple, nonradioactive, nontoxic in vitro assay to monitor corneal endothelial cell viability. *Invest Ophthalmol Vis Sci.* 1997;38(10):1929–1933.
38. Takasu Y, Yamada H, Tsubouchi K. Isolation of three main sericin components from the cocoon of the silk worm, *Bombyx mori*. *Biosci Biotechnol Biochem.* 2002;66(12):2715–2718.
39. Takasu Y, Yamada H, Tsubouchi K. The silk sericin component with low crystallinity [in Japanese]. *Sanshi-Konchu Biotec.* 2006;75:133–139.
40. Hu X, Shmelev K, Sun L, et al. Regulation of silk material structure by temperature-controlled water vapor annealing. *Biomacromolecules.* 2011;12:1686–1696.
41. Lee HK. Silk sericin retards the crystallization of silk fibroin. *Macromol Rapid Commun.* 2004;25:1792–1796.
42. Boettner EA, Wolter JR. Transmission of the ocular media. *Invest Ophthalmol.* 1962;1:776–783.
43. Beems EM, van Best JA. Light transmission of the cornea in whole human eyes. *Exp Eye Res.* 1990;50(4):393–395.
44. Connon CJ, Doutht J, Chen B, et al. The variation in transparency of amniotic membrane used in ocular surface regeneration. *Br J Ophthalmol.* 2010;94(8):1057–1061.
45. Kikkawa K. Biochemical genetics of *Bombyx mori* (silkworm). *Adv Genetics.* 1953;5:107–140.
46. Fedič R, Žurovec M, Sehnal F. The silk of Lepidoptera. *J Insect Biotechnol Sericol.* 2002;71:1–15.
47. Julien E, Coulon-Bublex M, Garel A, et al. Silk gland development and regulation of silk protein genes. In Gilbert LI, Iatrou K, Gill SS, editors. *Comprehensive Molecular Insect Science*, vol. 2. Amsterdam: Elsevier; 2005. p. 369–384.
48. Hogerheyde TA, Suzuki S, Stephenson SA, et al. Assessment of freestanding membranes prepared from *Antheraea pernyi* silk fibroin as a potential vehicle for corneal epithelial cell transplantation. *Biomed Mater.* 2014;9(2):025016.

49. Prausnitz MR, Noonan JS. Permeability of cornea, sclera, and conjunctiva: a literature analysis for drug delivery to the eye. *J Pharm Sci.* 1998;87(12):1479–1488.
50. Kato N, Sato S, Yamanaka A, et al. Silk protein, sericin, inhibits lipid peroxidation and tyrosine activity. *Biosci Biotechnol Biochem.* 1998;62(1):145–147.
51. Dash R, Acharaya C, Bindu PC, et al. Antioxidant potential of silk protein sericin against hydrogen peroxide-induced oxidative stress in skin fibroblasts. *BMB Rep.* 2008;41:236–241.
52. Nuchadomrong S, Senakoon W, Sirimungkararat S, et al. Antibacterial and antioxidant activities of sericin powder from Eri silkworm cocoons correlating to degumming process. *Int J Wild Silkmotl Silk.* 2008;13:69–78.
53. Fan JB, Wu LP, Chen LS, et al. Antioxidant activities of silk sericin from silkworm *Bombyx mori*. *J Food Biochem.* 2009;33:74–88.
54. Manosroi A, Boonpisuttinant K, Winitchai S, et al. Free radical scavenging and tyrosinase inhibition activity of oils and sericin extracted from Thai native silkworms (*Bombyx mori*). *Pharmac Biol.* 2010;48(8):855–860.
55. Isobe T, Ikebata Y, Onitsuka T, et al. Effect of sericin on preimplantation development of bovine embryos cultured individually. *Theriogenology.* 2012;78(4):747–752.
56. Lim KS, Kundu J, Reeves A, et al. The influence of silkworm species on cellular interactions with novel PVA/silk sericin hydrogels. *Macromol Biosci.* 2012;12(3):322–332.
57. Chlapanidas T, Faragò S, Lucconi G, et al. Sericins exhibit ROS-scavenging, anti-tyrosinase, anti-elastase, and *in vitro* immunomodulatory activities. *Int J Biol Macromol.* 2013;58:47–56.
58. Micheal AS, Subramanyam M. Influence of sericin in alleviating the hydrogen peroxide induced oxidative stress in silkworm *Bombyx mori*: role of the amino acids. *Invertebr Survival J (Modena).* 2014;11:257–272.
59. Prommuak C, De-Eknamkul W, Shotipruk A. Extraction of flavonoids and carotenoids from Thai silk waste and antioxidant activity of extracts. *Separ Purif Technol.* 2008;6(2):444–448.
60. Wang HY, Wang YJ, et al. Isolation and bioactivities of a non-sericin component from cocoon shell silk sericin of the silkworm *Bombyx mori*. *Food Funct.* 2012;3:150–158.
61. Butkhup L, Jeenphakdee M, Jorjong S, et al. Phenolic composition and antioxidant activity of Thai and Eri silk sericins. *Food Sci Biotechnol.* 2012;21:389–398.
62. Sangwong G, Sumida M, Sutthikhum V. Antioxidant activity of chemically and enzymatically modified sericin extracted from cocoons of *Bombyx mori*. *Biocatal Agric Biotechnol.* 2016;5:155–161.
63. Davies KJA. Oxidative stress, antioxidant defenses, and damage removal, repair and replacement systems. *Life.* 2000;50(4):279–289.